Counterintuitive active directional swimming behaviour by Atlantic salmon during seaward migration in the coastal zone

Matthew Newton[1], James Barry[1], Angus Lothian[1], Robert Main[2], Hannele Honkanen[1], Simon Mckelvey[3], Paul Thompson[4], Ian Davies[2], Nick Brockie[5], Alastair Stephen[5], Rory O'Hara Murray[2], Ross Gardiner[6], Louise Campbell[2], Paul Stainer[2], and Colin Adams [1]*

[1]Scottish Centre for Ecology & the Natural Environment, IBAHCM, University of Glasgow, Glasgow G630AW, UK
[2]Marine Scotland Science, Marine Laboratory, Aberdeen AB11 9DB, UK
[3]Cromarty Firth Fisheries Trust, CKD Galbraith, Reay House, Inverness IV2 3HF, UK
[4]Lighthouse Field Station, School of Biological Sciences, University of Aberdeen, Cromarty IV11 8YL, UK
[5]Scottish & Southern Energy, Inveralmond House, Perth PH1 3AQ, UK
[6]Marine Scotland Science, Freshwater Fisheries Laboratory, Perthshire PH16 5LB, UK

*Corresponding author: tel: +44 1360 870271; e-mail: colin.adams@glasgow.ac.uk.

Acoustic telemetry was used to track salmon smolts during river migration and into the open marine coastal zone. We compared migration direction and speed with particle tracking simulations to test the hypothesis that marine migration pathways are defined by active swimming current following behaviour. Habitat-specific survival rates, movement speeds, depths and directions in riverine, estuarine, and coastal habitats were also quantified. Salmon post-smolts did not disperse at random as they entered the unrestricted, coastal zone of the North sea; rather they chose a common migration pathway. This was not the most direct route to marine feeding grounds (ca. 44° N); north in the direction of the prevailing currents. Particle modelling showed that the actual post-smolt migration route was best predicted by active swimming at 1.2 body length.sec.$^{-1}$ at a bearing of 70° from north but not by current following behaviour. Fish migrating in larger groups and earlier in the migration period had increased migration success. We conclude that: post-smolts have preferred migration routes that are not predicted by the shortest direction to their ultimate destination; they do not simply use the current advantage to migrate; and that they actively swim, occasionally directly against the current prevailing at the time.

Keywords: anadromy, marine dispersal, migration cues, salmonid

Introduction

Long-distance migration is a highly risky strategy. The energetic costs directly incurred during the process of moving long distances are substantial (Dingle, 2014); the risks arising from navigation during migration and the uncertainty of finding suitable habitat of good quality and exploiting this resource following a successful migration are great (Rankin and Burchsted, 1992; Cresswell et al., 2011; Dingle, 2014) and the ecological adaptation required to be successful in the new environments are considerable (Alerstam et al., 2003).

The Atlantic salmon (*Salmo salar* L.) migrates from spawning and nursery grounds in freshwater rivers to feeding areas at sea, which include areas near the Faroe Islands and Greenland. The species is of considerable conservation value and supports important fisheries, mainly nowadays sport-fishing by rod and line. Currently, the numbers of adult salmon returning to freshwater

are declining, mainly as a result of reduced survival at sea (ICES, 2019). The migrating juvenile salmon face a broad range of challenges. If they are to be successful, they need to adapt to previously unknown habitats, very different ionic and osmotic conditions, unknown prey, novel predators and they need to do this whilst navigating through a set of unfamiliar environments to marine feeding sites that they have never visited before (Hoar, 1988; Rikardsen and Dempson, 2011). There are therefore good grounds for assuming that the earliest stages of seaward migration are likely to be a critical period in the life cycle of Atlantic salmon (Thorstad *et al.*, 2012).

Migration of salmon during the riverine phase of seaward migration has been well studied. However, there is relatively little accumulated empirical knowledge on the early marine stage of the life cycle of salmon. This is the result of the practical difficulties of studying salmon during transit from riverine to marine habitats. What evidence does exist indicates that mortality in the early marine stages of migration can be high. In their review of the existing studies, Thorstad *et al.* (2012) showed that the data suggest generally high, but also highly variable, mortality amongst smolts entering the near-shore marine environment. Mortality of up to 36% km^{-1} of migration has been reported in some estuaries, and averages ~6% km^{-1} in the early marine phase of migration (Thorstad *et al.*, 2012).

A second element of the migration into marine habitats by salmon that is poorly understood is the coastal migration pathways and the navigation cues used by smolts. The navigational requirements of the riverine migration component of seaward migration are relatively simple. The river channel constrains the need for complex navigation and studies have shown that smolts during seaward migration move with, and at a similar velocity to, the prevailing river current [see review in Thorstad *et al.* (2012)]. The potentially available directional navigation cues are considerably more diverse when smolts reach areas of standing waters (Honkanen *et al.*, 2018) once smolts reach the more complex coastal environments. The only data available for migration pathways around the UK come from limited information on smolt distribution at sea. Smolts were captured in the SALSEA-Merge study in surface trawls in the North Atlantic Ocean at relatively high concentrations in the Slope Current, which flows northeast along the continental shelf edge to the west and north of Scotland and Ireland (NASCO, 2011). These data indicate that many smolts migrated by this route to a staging area in the Norwegian Sea prior to moving on to other parts of the North Atlantic including feeding areas near the Faroes and Greenland before eventually returning to home waters. However, these data only provide a coarse resolution picture of migration routes and little information on the cues to navigate these routes, although the results were found to be consistent with active swimming that is aligned with the surface current. What evidence there is thus suggests that salmon post-smolts are showing swimming-augmented, current following in the first few months of sea migration in the North-East Atlantic (Mork *et al.*, 2012; Ohashi and Sheng, 2018; Chaput *et al.*, 2019). Similar studies have not been conducted in the North Sea and therefore no information is available on whether salmon smolts in this area are responding similarly to cues. Additionally, it is not known if smolts emanating from rivers draining into the North Sea join the migration pathways of those from the western coasts of the British Isles or whether they take a more direct route to the same staging area in the Norwegian Sea. More recently chinook salmon (*Oncorhynchus*

tshawytscha) have been shown to use inherited "magnetic maps" to aid their navigational abilities (Putman *et al.*, 2014). Similarly, Minkoff *et al.* (2020) have shown that Atlantic salmon appear to be able to use magnetic maps to aid in their navigation. Some authors also suggest salmon actively migrate using celestial cues (Hasler, 1966; Quinn *et al.*, 1989). Thus Thorstad *et al.* (2012) conclude that there are likely to be complex combinations of cues and senses that are utilized by migrating fish to determine their direction of travel in coastal zones and the open sea.

The use of electronic acoustic transmitters is a proven and effective technology for detecting movement and migration of aquatic species in coastal, estuarine, and freshwater ecosystems (Cooke *et al.*, 2004, 2013). The development of telemetry and the insights that it brings have been reviewed extensively (Lucas and Baras, 2000; Hodder *et al.*, 2007; Halttunen *et al.*, 2009; Cooke and Thorstad, 2011; Hussey *et al.*, 2015). Briefly, acoustic telemetry requires a transmitter, attached to an individual animal, which transmits a coded sonic signal to a receiver comprising of a hydrophone and a data logger. Acoustic tags are uniquely coded, but are also able to determine and send information to the receiver on the environmental parameters (e.g. depth and temperature) being experienced by the fish at the precise moment of transmission. Telemetry information can therefore be used to determine the position of the tagged individual at a specific time and provide environmental and physiological data on that fish (Thorstad *et al.*, 2013). By deploying receivers at various positions in the study system, it is possible to monitor the behaviour and survival of migrating tagged fish.

The general aim of the study presented here was to gather new information on the migration of salmon smolts as they transit from a river that drains into the North Sea on the east coast of Scotland (the River Conon), through a marine estuary (the Cromarty Firth), to a relatively open coastal zone (the Moray Firth) in an area where there is very little information on migration passage routes in general. More specifically this study tested the premise that salmon post-smolts migrating into the North Sea are showing "augmented current following" (cf. Mork *et al.*, 2012). Thus, that their direction of travel is predicted by water current direction but that the speed of travel would be greater than the current speed. In addition, a number of subsidiary aims were addressed. These were to estimate the rate of mortality and the speed and timing of movement of salmon smolts during lower river, estuary, and early marine migration phases of migration to the open sea.

Methods
Study area
The Moray Firth 57.9783°N 002.9650° W forms the largest single marine embayment of the North Sea on the east coast of Scotland (Figure 1). It is meso-tidal, with a relatively uniform tidal range of <3.5 m around its coastline (see Hansom and Black, 1996).

The Cromarty Firth, 57. 6817°N 004.2117°W, is the major estuary discharging into the west of the inner Moray Firth (Stapleton and Pethick, 1996). The Cromarty Firth is the freshwater to marine estuarine transition zone for the River Conon catchment, which discharges at the head of the relatively narrow firth. The ca. 18 km long Cromarty Firth widens from west to east through two relatively broad tidal bays, Udale and Nigg bay, but then narrows (to 1.25 km) between the North and South Sutors before discharging into the inner Moray Firth. There is a single,
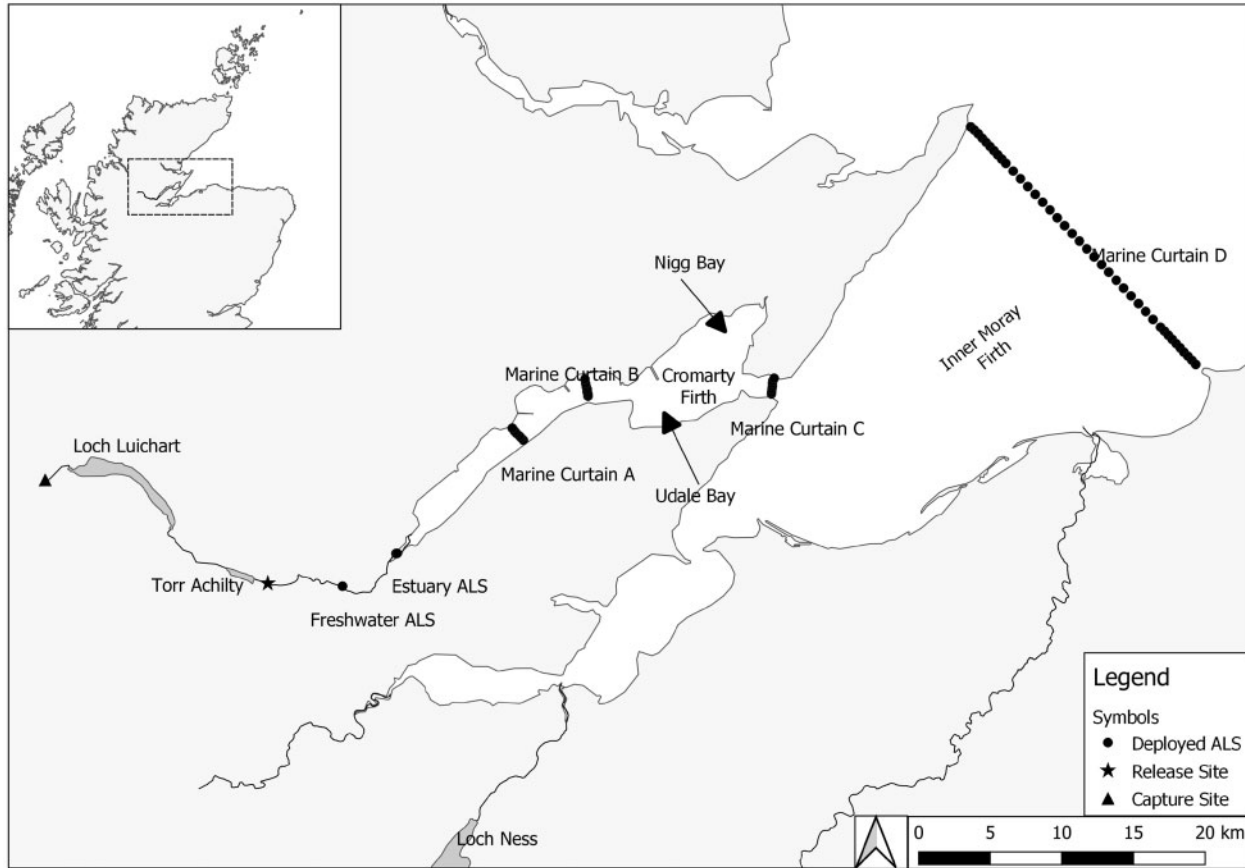
Figure 1. Top left: The location of the wider Moray and Cromarty Firths, North East Scotland. Main Figure: Deployment locations of ALSs showing individual acoustic receiver curtains and Atlantic salmon smolt capture and release sites.

relatively deep (ca. 15–20 m), glaciated trench of about 1–1.5 km width that approximately follows the midline of the firth.

Smolt capture and tagging

Atlantic salmon smolts ($n = 120$) were captured in a fixed Wolf trap in a tributary of the River Conon, 33 km upstream from the Cromarty Firth (Capture site, Figure 1). Fish greater than 130 mm fork length and which were also clearly smolting (Eek and Bohlin, 1997; Sloat and Reeves, 2014) were anaesthetized with clove oil (0.5 mg L^{-1}) and measured for mass (M, g), fork length (L_F, mm), and whole body lipid density (%) (Distell fish fat metre FM 692) prior to tagging. For this, fish were placed on a v-shaped surgical pillow saturated with river water and an incision of 11–14 mm length was made along the ventral abdominal wall anterior to the pelvic girdle. A 69 kHz coded acoustic transmitter (Model LP-7.3, 7.3 mm diameter, 18 mm length, 1.9 g mass in air, Thelma Biotel AS, Trondheim, Norway) was inserted into the peritoneal cavity. The incision was closed with two independent sterile sutures (6-0 ETHILON, Ethicon Ltd, Livingston, UK). Fish were irrigated with 100% river water throughout the procedure. Tags were programmed for an acoustic transmission repeat cycle of 25 s ± 50%, giving a tag life of in excess of 90 d. The acoustic tags also transmitted data on the depth and temperature of the tag every 25 s ± 50%. Depth measurements had a resolution of 10 cm up to a maximum depth of 25.5 m; temperature measurements to ±0.5°C.

Tagged fish were placed in a bucket filled with aerated river water and allowed to recover. Fish were then transported downstream (20 river km) to the release site (Figure 1: Smolt Release site), 13 km upstream from the tidal limit of the Cromarty Firth. Trapping and transport of migrating smolts are routinely conducted by the Cromarty Firth District Salmon Fishery Board (CDSFB) as an impoundment mitigation measure (Figure 1). Tagging of smolts with passive integrated transponder tags in this system has routinely demonstrated return rates of adult fish of around 3–6% (S. Mckelvey, pers. comm.). Fish tagged with acoustic transmitters were released into the river in a small, calm eddy in the River Conon at the same time as untagged fish were released ∼200 m upstream. Untagged fish were not used for any analysis within this study. All procedures were conducted under UK Home Office Licence PPL 70/8794.

Acoustic tracking

Movement of tagged smolts was determined by using acoustic receivers at fixed position automatic listening stations (ALSs) (Vemco VR2W, VR2Tx, or VR2-AR). All ALSs were deployed prior to the commencement of fish tagging. One ALS, a VR2W, was positioned in the lower reaches of the River Conon upstream of the tidal limit (FW on Figure 1). Similarly, a gate of two ALSs (VR2Ws) was positioned in fresh water at the upstream tidal limit of the River Conon at the upstream limit of the Cromarty Firth Estuary (marked "Estuary ALS" on Figure 1). Twenty VR2Tx

receivers were positioned in three transverse curtains (*sensu* Heupel *et al.*, 2006) crossing the Cromarty Firth. ALS's within marine curtains A, B, and C were spaced on average 205 m apart. Marine Curtain D (Figure 1) comprised of 40 VR2AR, ALS's within 5 km from either shore were spaced at 400 m intervals, increasing to 750 m spacing further offshore. All ALSs remained in place until 22 August 2016, at which time all fish would have migrated and the expected life expectancy of the tags would have passed. All ALS's were deployed subsurface and without surface markers to reduce any additional anthropogenic noise, thus promoting the probability of detecting tagged fish.

Range testing

Range tests were undertaken prior to deployment of the final array for Cromarty Firth ALS curtains. Two curtains of six receivers were deployed for 1 week in the vicinity of marine curtains A and C. Locations were selected to be representative of planned final array positions. The data obtained indicated an acoustic detection efficiency in excess of 75% at 200 m. Receivers were therefore deployed to create overlap in the detection ranges of ALSs at this distance. "Sync tags" comprising transmitters built into each VR2Tx and VR2AR ALSs (i.e. at each of the four curtains) were programmed to transmit with a power output equivalent to 142 dB re 1μPa at 1 m depth on all receivers to enable detection efficiency testing, which remained high throughout the study period with detections at distances in excess of 800 m.

In addition, detection efficiency of curtain C was further tested. An acoustic tag (model LP-7.3, 139 dB re 1μPa at 1 m, Thelma Biotel AS, Trondheim, Norway) was suspended at 3 m depth and allowed to drift, at approximately maximum distance, between each ALS to test for the non-detection of a transmitter as it transited through the receivers (an acoustic breach). No acoustic breach (that is a non-detection of the transmitter) occurred during these tests. Tag failure rate reported by the manufacturers is low (<2%) and Gauld *et al.* (2013) reported failure rates for the same tags of 0% in a field test.

Fish migration behaviour

Fish migration behaviour was inferred from the pattern of detections of tags at, and between, the fixed position ALSs. Two principal measures of behaviour were quantified in this study. A "residency event" was defined as at least two consecutive detections of a fish at an individual gate or curtain (Campbell *et al.*, 2012; Breece *et al.*, 2018). A residency event begins when either a tag was detected at an ALS curtain where it had not been detected previously or where it had not been detected at that curtain for a period of greater than 60 min. Thus, any individual fish may be recorded as having multiple consecutive residency events at a single curtain if they occur more than 60 min apart. A residency event will thus have a location and duration associated with it. Tag depth was also determined during a residency event as the mean depth of a tag during a single residency event of any length.

A "movement event" was defined as the period between two residency events where the tag is detected at different curtains. Each movement event had four measurable variables associated with it. A movement "direction" was simply defined as either seaward (i.e. towards the open sea, downstream) or landward (in the opposite direction, upstream). A movement "duration" was determined as the time from the end of one residency event to the start of the next. The "distance travelled" between curtains C and

D was determined using the straight-line distances between the individual ALSs where the tag was detected. For all other array pairs, distance travelled was taken to be the distance between the curtains measured along the centre line of the river/estuary using QGIS software.

The rate of movement (ROM) was determined as the ground speed of an individual between two curtains calculated as the distance between receivers divided by the time difference between the last detection at one curtain and the first detection at the second. The design of this study did not allow for the exact route taken by a fish between curtains to be determined (only the direct, and thus minimum, distance travelled) therefore both distance travelled, and ROM must be regarded as minimum values of these metrics.

Confirmed survival (i.e. successful migration) was determined by detection of individuals at successive seawards receivers. It was assumed that fish, which were detected at an upstream receiver but not at the subsequent downstream receiver, were lost to the study within that intervening area. Losses are reported as % km^{-1} to enable comparisons between sites and studies.

Environmental data

Meteorological data were obtained from a weather station located at Tain Range (57.8167°N 003.9667°W) ~14 km north of the study site (Figure 1). Tidal height data were provided by the Scottish Environment Protection Agency (SEPA) from a monitoring station adjacent to the Cromarty Firth. The timing of sunrise and sunset were calculated using the "maptools" package in R (Bivand and Lewin-Koh, 2016; R Core Team, 2016).

Tag detection efficiency

Since there is potential that some tagged fish were not detected as they passed an ALS curtain, interpreting detection as the total survival of tagged fish may be confounded by the probability of transmitter detection. Knowledge of detection probability is therefore essential in obtaining unbiased estimates of the survival rate of migrating smolts.

There are several strands of evidence from this study that indicate detection rates of passing fish are high. Transmissions from sync tags were detected at distances in excess of 400 and 800 m, although efficiency reduced with distance. Thus, detection of fish passing through each of the three curtains in the Cromarty Firth was possible by two or more receivers. Where there were receiver curtains in a seaward direction from any curtain of interest, curtain efficiency can be estimated from fish detected at subsequent curtains but not at the one of interest. For curtain D, where additional downstream receiver curtains are not available, it is possible to estimate the potential detection error from known detection efficiency data. Detection efficiency estimates made at curtain D were used to model the likelihood of a smolt migrating through a receiver curtain without detection. Simulations were based on the method proposed by Hayden *et al.* (2016). Virtual fish are "swum" at a receiver line, a simulated signal from a tag is transmitted randomly with intervals of between 15 and 45 s (as per tag spec in this study). The distance between transmission location and each receiver is calculated. A detection range curve is then used to calculate the probability (p) that the signal was detected on each receiver. Detection or non-detection at each receiver is determined by drawing from a Bernoulli distribution with a probability of p. Detection range curves were calculated

from sync tags [Model LP-7.3, 7.3 mm diameter, 18 mm length, 1.9 g mass in air, Power output (dB re 1 uPa at 1 m) 139 decibels, Thelma Biotel AS, Trondheim, Norway] positioned within the coastal marine curtain. Detection probabilities were calculated for 3-h periods during the time when fish were actively migrating across the curtains and used within the simulations (Hayden *et al.*, 2016).

Statistical modelling

Four models were constructed to examine possible drivers of migration behaviour in this study. *Model 1*: The mean ROM for each movement event was modelled as a response to four potential explanatory variables: movement location [the pair of curtains between which the movement event occurs (*n* range 19–86)], wind speed, fish fork length (L_F) and fish body lipid content using a generalized linear mixed effect model (GLMM), for Gamma distributed data. Other possible variables: fish mass and tag mass: body mass ratio were not included because they were all strongly correlated with fish L_F and thus violated collinearity criteria for inclusion. Fish tag number was included as a random factor to account for repeated measures. Between-group *post hoc* tests were conducted by Tukey's HSD. *Model 2:* The duration for each residence event was regressed against five explanatory (fixed) variables [tide state (ebb or flood), mean swimming depth, lipid content, F_L, and curtain] using a GLMM for Gamma distributed data. Fish tag number was included as a random factor to account for repeated measures. *Model 3*: The proportion of within group survival, that is the confirmed survival rate of a group of smolts released on any one day, defined as the total number that survived to the coastal marine curtain (D) as a proportion of the number in the group, was modelled using the day of year at release (DOY), and the total number of fish in the release group in a logistic regression model for binomial distributed data. Explanatory variables were treated as fixed effects. A *group* refers to the number of tagged fish released at any one time; the number within the group reflects a subsample of the population of fish migrating on that day (for numbers see Supplementary material). *Model 4*: Confirmed survival (Yes or No) measured as detection of a tag at the coastal marine curtain (curtain D) was modelled as a binary response to five potential explanatory variables: fork length (L_F), ROM measured through Cromarty Firth (ES to SU), fish lipid content, DOY, total number of fish within release group. All explanatory variables were treated as fixed effects.

For all models, a maximal model with all fixed effects included was created. A minimum model was then derived using the top down strategy as described by Zuur *et al.* (2009) with the elimination of non-significant explanatory terms. Stepwise significance testing between nested models was conducted in ANOVA. The final model contained only the significant predictors of the response variables. Pseudo R^2 values for models generated without a gamma distribution were calculated using the *r*-squared GLMM function in the MuMln package (Bartoń, 2016).

Particle tracking

To test the hypothesis that migrating post-smolts are actively swimming with the prevailing current (*sensu* Mork *et al.*, 2012), a particle tracking model was used to explore where passive, neutrally buoyant, particles released in the Cromarty Firth would travel under the influence of the natural hydrodynamics in the Moray Firth region and subsequently to test other models of

passage such as augmented current following. The particle tracking model was forced by a hydrodynamic model of the Moray Firth previously developed by Marine Scotland Science (Campbell, 2018). The model has 10 terrains following vertical layers, each representing 10% of the water column, and an unstructured computational grid with individual node spacing varying from 60 m in some inshore areas to 2.6 km at the mouth of the Moray Firth. The node spacing within the Cromarty firth particle release zone was around 150–200 m. For the purpose of the present study, the model was run for the period March—August 2016. The hydrodynamic model was based on the Scottish Shelf Model (SSM) (Wolf *et al.*, 2016; De Dominicis *et al.*, 2018). The SSM is a high resolution hydrodynamic model of the wider Scottish Shelf and is an implementation of the Finite Volume Community Ocean Model (FVCOM) (Chen *et al.*, 2003). The Moray Firth model was forced at the boundary by data from the Atlantic Margin Model at 7 km resolution, which is an operational forecast model run by the UK Met Office (Edwards *et al.*, 2012; O'Dea *et al.*, 2012). The forcing parameters at the boundary were current speeds, water elevation, temperature, and salinity. The wind and atmospheric properties for the model were forced by modelled data from the European Centre for Medium Range Weather Forecasts (ECMWF) ERA-Interim reanalysis (Dee *et al.*, 2011). The freshwater river input for the model used here included five dominant rivers (Conon, Ness, Findhorn, Spey and Deveron; Figure 1). The river discharge data were provided by the Scottish Environment Protection Agency and the National River Flow Archive (https://nrfa.ceh.ac.uk/) for the appropriate gauging stations in these rivers during the time of interest.

The Lagrangian particle tracking model used has recently been upgraded to enable additional horizontal advection of particles, representing configurable behaviour, by Ounsley *et al.*, (2019). The code builds on the FISCM software originally developed for FVCOM output by Liu *et al.* (2015) and solves a non-linear system of ordinary differential equations in order to update the particle position as it changes with time due to the hydrodynamic environment. A more detailed description of the Lagrangian particle tracking model is given by Chen *et al.*, (2011) and Liu *et al.* (2015).

Particle tracking modelling was used to simulate potential behaviour and pathways smolts might be using to navigate in the coastal environment. A variety of simulations (Table 3) were used to cover a variety of possible biological factors. PT1 models had passive particles, i.e. drifting with currents exhibiting no biological behaviour. This model would predict the direction of passage (although not the speed) of fish exhibiting augmented current following. PT2 models comprised directed swimming scenarios with specific bearings [at 60°, 70°, 80° 90° from North in a clockwise direction (PT2.1 to PT2.4)]. PT3 models had directed swimming in the opposite direction to the currents in order to simulate negative rheotaxis (Table 3), with PT3.1 forcing particles to behave in this manner continuously throughout (regardless of the phase of the tide). Some variations of PT3.1 were also explored with PT3.2 and PT3.3, where directed swimming was turned on/off depending on the direction of the currents (i.e. ebb or flood tide). To simulate the effects of directional swimming in addition to current effects on pathways used by smolts, theoretical particles were given a swimming speed of 0.168 m s^{-1}, a speed derived from smolts with a fork length of 140 mm (in the middle of the range of smolts in this study) swimming at 1.2 body lengths per second (bl s^{-1}) relative to the water, which Thorstad *et al.*

(2004) give as a typical value for migrating post-smolts. To implement the particle tracking simulations, the particle trajectories were a function of deterministic flow fields from the hydrodynamic model and particle behaviour, and stochastic dispersion (random walk diffusion). For this stochastic component of dispersion a horizontal diffusivity (controlling the rate at which particles randomly spread horizontally using a random walk scheme) of $10\,\text{m}^2\,\text{s}^{-1}$ was applied in all of these experiments as this has previously been deemed to be representative of Scottish waters in general (Okubo, 1971). These experiments are likely to be dominated by the deterministic flow fields and behaviour rather than the stochastic component and the diffusivity value chosen is unlikely to have a strong baring on the results.

For each particle tracking model run, a total of 1000 particles were released at the surface from 10 locations/time combinations at curtain C, 100 particles from each location/time. These release locations/times were determined by actual detections of individual smolts at curtain C. Particle releases were made at 57.6826° N, 004.0015° W where four smolts were detected, at 57.6899° N, 004.0005° W where two smolts were detected, and at three other locations (57.6864°, 004.4.0008° W; 57.6813° N, 004.0017° W; 57.6864° N, 004.0008° W) at each of which one smolt was detected. The particle release times were between 23 April and 19 May. The particles were released, and forced to stay, at the surface where they were subject to the deterministic flow fields modelled by the top hydrodynamic vertical layer representing the top 10% of the water column. The particles were not subject to vertical advection either by the hydrodynamics or stochastic diffusion. This was because the tag depth data showed that the smolts stayed in the top 5 m of the water column.

Results

Acoustic tracking
In total, 120 downstream migrating Atlantic salmon smolts were tagged with acoustic tags and released during the study (Supplementary Table S1). These fish had a mean fork length (L_F) of 144.3 ± 6.7 mm *SD*, a mean mass (M) of 29.4 ± 4.2 g *SD*, and mean lipid level of 2.7 ± 1.2% *SD*. Fish were detected on every curtain within the study area; there were 59 248 detections of tags from study fish and >1 500 000 detections of sync tags. Fish were detected at the first ALS in the array (FW) on average 3.9 ± 5.3 *SD* days after release (distance from release site to FW ALS = 6.1 km). Detection of a fish at the FW ALS confirmed its downstream migration. Subsequently, movement was generally rapid, taking on average 8.1 ± 3.5 (mean ± *SD*) days to travel the ca. 62 km from the most upstream ALS to the outer curtain D (Figure 1); a minimum travel speed of 7.7 km.d^{-1}. Despite tagging and releasing fish over a period of around 30 d, the majority of fish (80.3%) passed through curtain D within a 10-d period (31 April to 9 May).

Direction of travel
Progress through the Cromarty Firth was largely downstream and seaward to the open coast with 90% of all recorded movements (total $N = 185$) in this direction. All landward (upstream) movements recorded in the firth occurred between curtains A and B. Of the 83 fish detected at curtain B, 19 (22%) were re-detected at curtain A before exiting the firth. Three of these 19 individuals

(16%) exhibited this behaviour twice, thus transitioning between curtains A and B five times prior to exiting the firth.

Fish were detected across all ALSs within each of the three curtains in the Cromarty Firth with no clear route preference across curtains. This was not the case, however, for curtain D. Here, a clear a route preference was observed with fish detected predominantly on the south-eastern ALSs. Of the 56 fish detected on curtain D, 39 (69.6%) were detected within 6 km from the south-eastern shore of the Moray Firth (Figure 2). No detections of tagged fish occurred on the north-western 6 km of the curtain. Five fish recorded more than one residence event at curtain D.

Confirmed survival
The confirmed survival of fish tagged in the River Conon seaward to curtain D was 46.7% (56 of 120) (Figure 3) at a total loss rate (across the whole of the migration route examined in this study) of 0.69% km^{-1}. More specifically, escapement differed across the four principal habitat types. River escapement (freshwater to estuary) was 73.3% ($n = 88$ of 120) at a loss rate of 2.2% km^{-1}. Estuarine escapement (estuary receiver to curtain A) was 95% ($n = 84$ of 88) at a loss rate of 0.37% km^{-1}. Firth escapement (curtain A to curtain C) was 94% ($n = 79$ of 84) at a loss rate of 0.32% km^{-1}. Early marine escapement (Curtain C to Curtain D) was 71% ($n = 56$ of 79) at a loss rate of 1.2% km^{-1}. Thus, relative loss rate (Table 1) was highest between the release site and FW receivers (3.1%/km loss rate) followed by marine migration between Curtain C and Curtain D (1.2%/km).

Three fish were not detected at curtain C, which were subsequently detected at curtain D. This is a detection error rate of 3.9% for this curtain. These three fish are included within the analysis and survival estimates since they were detected at curtain D. No other fish were detected at a seaward curtain, which had not been detected at the preceding landward curtain. On average, fish had 19 ± 21 detections (mean ± *SD*) at curtain D; thus the complete lack of detection of a fish adds credibility to the inference of loss as opposed to non-detection.

Model simulations were conducted to determine the probability of a fish transiting curtain D without being detected. Ten thousand individual simulations comprising 79 fish (the total number detected passing through the previous curtain (C)) swimming randomly at the entire length of the curtain D at speeds between 0.6 and 1.4 ms^{-1} [the maximum ROM between curtain C to curtain D and between FW and the estuary ALS (Figure 1) (i.e. fastest travel speeds)] were run. Transmitted signal interval was allowed to vary randomly between 15 and 45 s to simulate the tag settings in this study. The model thus incorporated realistic variables at the top of the range of data recorded and thus were likely to yield a maximum estimate of undetected fish (i.e. a worst-case scenario). The mean [± standard deviation (*SD*)] proportion of simulated fish that were detected across the 10 000 simulations was 0.97 ± 0.03. Given that 56 fish were detected at the coastal marine curtain, these simulations indicated the potential that two (1.68) additional fish may have passed curtain D without being detected thus potentially increasing confirmed survival by 2.4%In another simulation to investigate the effect of swimming speed on detection probability, it was found that fish would need to swim in excess of 1.7 ms^{-1} to reduce detection probability to <0.9.
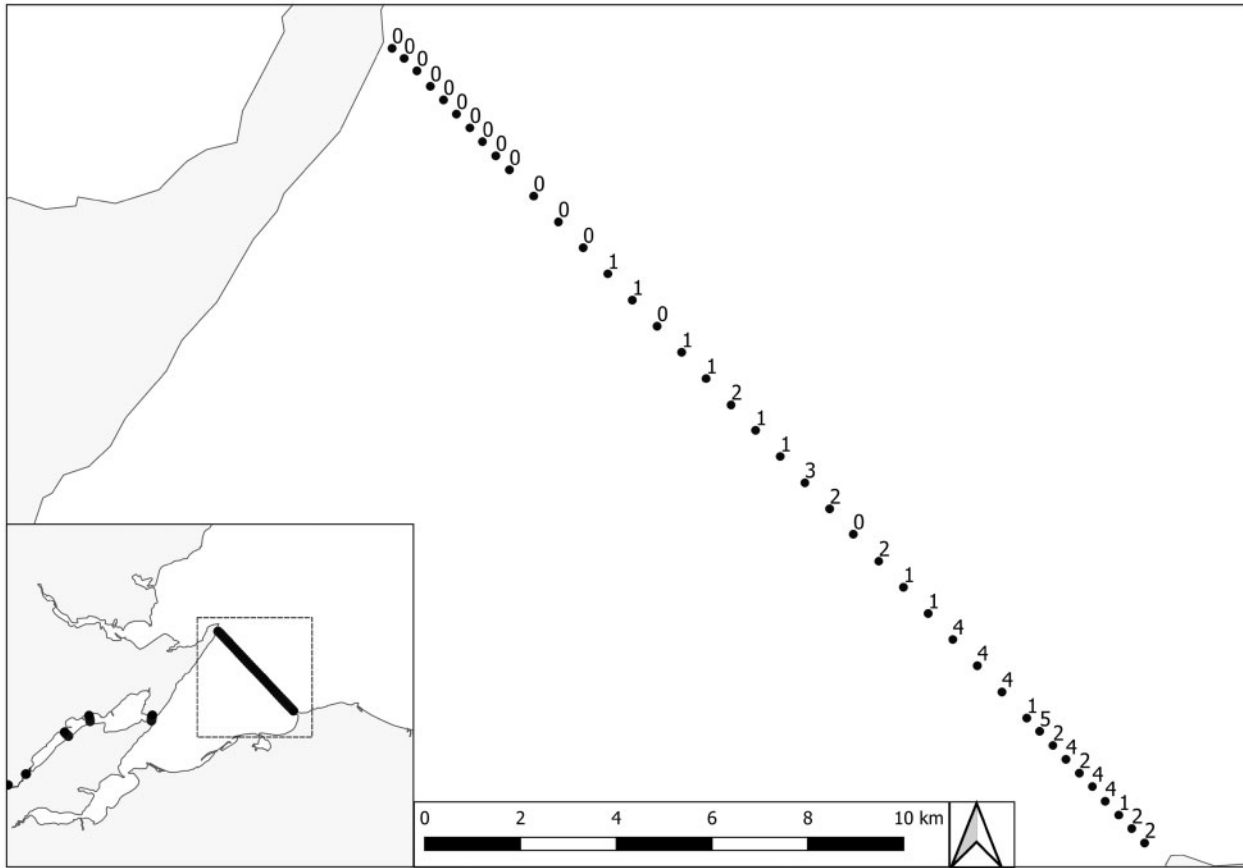
Figure 2. The numbers of first detections of fish by individual ALSs along the Coastal Marine curtain (Curtain D; Figure 1).
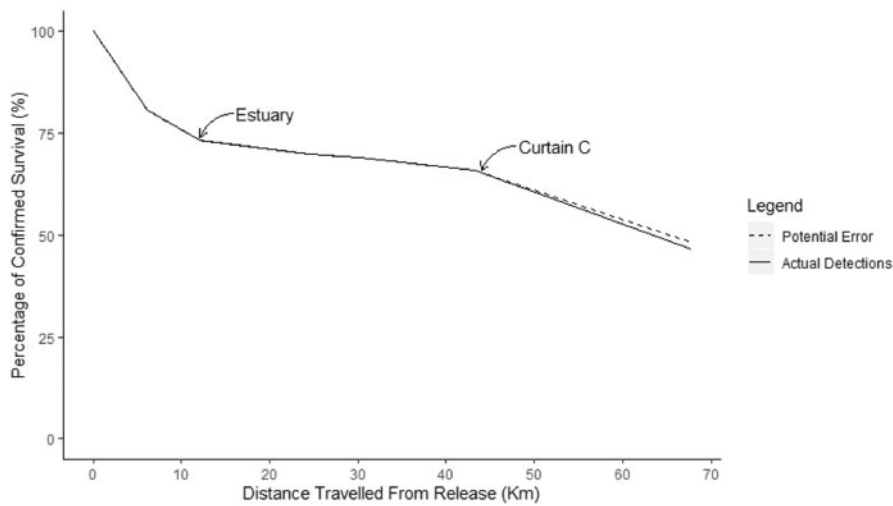

Figure 3. The proportion of the tagged smolts detected on the migration route through river, estuary, and coastal marine habitats. The possible likely maximum number of undetected fish at the last curtain (C) is derived from simulations described in the text and is indicated by the dashed line.

Swimming depth

Swimming depth of a fish was calculated as the mean depth of detections (as indicated by the acoustic transmitter) for each fish during each residence event at each curtain. Fish exhibited a significant diurnal effect in their swimming depth. In fresh water and estuary, fish were significantly deeper (Wilcoxon, $W = 2417.5$, $p \leq 0.005$) at night (mean $= 2.53 \pm SD$ 0.75 m) than during the day (mean $= 1.74 \pm SD$ 0.77 m). In saline

Table 1. Mean and SDs of rates of movement and the duration of fish moving between each curtain.

Movement location	Mean ROM ms^{-1}	SD ROM ms^{-1}	Mean duration (h)	SD duration (h)	Loss per km (%)
Release - > FW ALS	0.08	0.09	90.69	127.11	3.14
FW ALS - > estuary ALS	0.26	0.38	46.32	54.76	1.55
Estuary ALS - > Curtain A	0.13	0.15	52.79	43.77	0.37
Curtain A - > Curtain B	0.53	0.34	6.63	15.02	0.21
Curtain B - > Curtain A *	0.62	0.13	2.50	0.68	0.00
Curtain B - > Curtain C	0.29	0.30	25.45	22.04	0.37
Curtain C - > Curtain D	0.27	0.14	37.39	20.84	1.18

*Landward movement from curtain C to B.

environments (curtains: A, B, C, D), fish were significantly (Wilcoxon, W = 25074, $p \leq 0.005$) shallower during the night (mean = 0.56 ± SD 0.56 m) than in the day (mean = 1.03 ± SD 0.62 m). Throughout the Cromarty Firth and Moray Firth migration, fish were predominantly recorded within the top metre of the water column (mean = 0.8 ± SD 0.6 m), although fish were recorded throughout the top 5 m of the water column. One individual reached the maximum depth that can be recorded by the tag recording of 25.5 m at curtain C. This individual was removed from depth analysis at the curtain C array due to the exact depth of the fish being un-identifiable. The fish was subsequently detected at curtain D at <5 m depth. Fish were also deeper during a flooding tide (mean ± SD, 0.87 ± 0.67) than during an ebbing tide (mean ± SD, 0.77 ± 0.2) although the absolute difference in depth was small and not significantly different.

Model 1: ROM
The ROM during movement events was significantly predicted by two variables. The final model accounts for 25.0% of variation in the data, 24.6% of this variance is explained by where the movement occurred (i.e. between specific curtains) ($\chi^2_5 = 111.38$, $p \leq 0.001$) and 0.4% of variation is explained by wind speed ($\chi^2_1 = 5.61$, $p = 0.002$), with higher windspeeds increasing ROM. Fish fork length is close to statistical significance ($p = 0.056$), with length having a slight positive effect on ROM.

A *post hoc* Tukey's test showed that the ROM differed significantly ($p < 0.05$) between migration zones. Movement between curtains A and B was the most rapid and significantly different from all other movements. This held true for movements in both the "upstream" and "downstream" movements at this location.

Model 2: Residence event duration
The mean duration of a residence event for fish at an individual ALS was significantly predicted ($\chi^2_2 = 46.65$, $p \leq 0.001$) by the additive effects of tidal state ($\chi^2_1 = 27.60$, $p \leq 0.001$) and mean depth of the fish ($\chi^2_3 = 14.91$, $p \leq 0.001$) during the residence event. Mean residence of fish within the range of an ALS was significantly higher when the residence event occurred during a flooding tide (mean = 27.9 ± 50.44 SD min) as opposed to an ebbing tide (mean = 15.28 ± 30.45 SD min).

Model 3: Group survivorship
The proportion of within-group tag detection to curtain D was significantly predicted by both DOY and the total number of individuals within the release group (Table 2). The odds ratio and model summary indicate that as DOY of release increases, survival decreases, and as group number increases so does survival.

Table 2. Beta, standard error, and confidence intervals for a logistic regression model, which predicts the survival rate of each group of smolts.

| | B (SE) | 95% CI for odds ratio | | |
		Lower	Odds ratio	Upper
Constant	7.8 (3.9)			
DOY	−0.07 (0.03)	0.87	0.93	0.99
Group number	0.03 (0.02)	0.99	1.03	1.08

This is also an additive effect in that larger groups migrating earlier in the migration period have better survival than larger groups migrating later in the migration period. A model with an interaction between DOY and number of individuals had less statistical support than the additive model.

Model 4: Individual survival
None of mean fork length (L_F), ROM through Cromarty Firth (calculated from ES to SU), fat content, DOY of release, or total number of fish in the release group significantly predicted detection of an individual smolt through the study area. Thus, although it is possible to predict the probability of survival of a group, it is not possible to predict survival of individual fish within the specific group.

Particle tracking
Each particle tracking simulation modelled the release of particles at curtain C. For each trial, the location and time that each particle first crossed curtain D, and the transport duration was recorded. Thus, results formed a distribution of crossing locations along curtain D. The particle tracking simulation, the mean transport durations (between curtain C and D), and some comments regarding the distribution of crossing locations are summarized in Table 3. Figure 4 shows output from PT2.2 where each particle was given a swimming behaviour comprising a constant speed of 0.168 m s^{-1} on a bearing of 70° from N. Curtain D crossing points are distributed along the south-eastern two-thirds of the curtain, with by far the most crossings occurring at the south-eastern end. This distribution is typical of most of the particle tracking experiments performed, with no particles ever crossing towards the north-western end of the curtain during simulations PT2 and PT3. For PT1 (passive particles, indicative of the route that would be taken under the assumption of augmented current following), there was a more even distribution across the curtain, which did not match the pattern shown by fish passage.

Table 3. Particle tracking simulations performed and the mean duration of particles to travel from their release location on Curtain C (Figure 4) to Curtain D (Figure 1).

|	Behaviour	Mean duration (h)	SD duration (hours)	Distribution of crossing locations at Curtain D
PT1	Passive particles	132	103	Particles distributed along transect with highest concentration at the south-eastern end
PT2.1	Constant advection speed of 0.168 m s^{-1} at a bearing of 60° from N	39	55	Crossing points distributed across the south-eastern two-thirds of the transect, with most particles approximately in the middle of the transect
PT2.2	Constant advection speed of 0.168 m s^{-1} at a bearing of 70° from N	41	48	Crossing points distributed across the south-eastern two-thirds of the transect, with most particles crossing at the south-eastern end
PT2.3	Constant advection speed of 0.168 m s^{-1} at a bearing of 80° from N	76	116	Most particles cross at the south-eastern end
PT2.4	Constant advection speed of 0.168 m s^{-1} at a bearing of 90° from N	175	189	All particles cross at the south-eastern end
PT3.1	Negative rheotaxis with speed of 0.168 m s^{-1} at all times	101	88	Crossing points distributed across the south-eastern two-thirds of the curtain, with the majority of particles crossing at the south-eastern end
PT3.2	Negative rheotaxis with speed of 0.168 m s^{-1} only when eastern velocity > 0 m s^{-1}.	126	98	Crossing points distributed across the south-eastern two-thirds of the curtain, the majority of particles crossing at the south-eastern end
PT3.3	Negative rheotaxis with speed of 0.168 m s^{-1} only when easterly velocity >0 m s^{-1} and northerly velocity >0 m s^{-1}.	109	84	Crossing points distributed across the south-eastern two-thirds of the transect, the majority of particles crossing at the south-eastern end
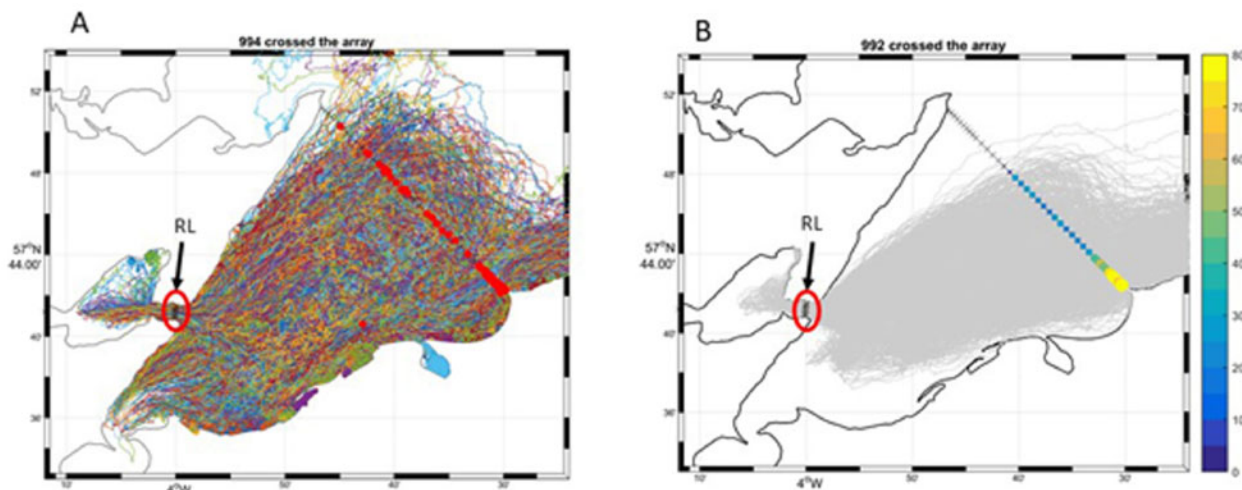
Figure 4. The output from two particle tracking models comprising 1000 particles released from 10 locations (shown as RL). Lines denote individual particle paths. (a) Model PT1, particles are passive in this model (i.e. drifting with the current, exhibiting no biological behaviour). The direction of travel (but not the time of travel) in this model is equivalent to augmented current following. Mean time to crossing receiver curtain D: 5.5 ± 4.3 d. The red points indicate the locations of particles crossing marine curtain D. (b) Model PT2.2 in this model particles were modelled as actively swimming on a bearing of 70° (clockwise from north) at 0.168 m s^{-1} (equivalent to 1.2 bl s^{-1} for a 140 mm length fish). Yellow colouration indicates more particles, green intermediate number and blue, fewer particles crossing curtain D. Mean time to reach curtain D under these conditions was 1.7 ± 2.0 d. This model best represented both the direction and timing of travel of fish in this study.

Most of the particle tracking simulations produced the observed pattern of most of the smolts crossing the south-eastern end of curtain D. The only simulation that did not produce this result was PT2.1 where a constant bearing of 60° was imposed on the particles, forcing them to cross the transect further north. There was a wide variation in the duration that the particles took to travel from curtain C to curtain D between simulations. Most

of the particle tracking simulations produced mean durations much longer than the observed time of 37.39 ± 20.84 *SD* h taken by tagged smolts (Table 1), but PT2.1 and PT2.2 had very similar mean durations of 39 ± 55 *SD* h and 41 ± 48 *SD* h, respectively. Of all the models tested PT2.2 with a constant bearing of 70° at 0.168 m s^{-1} produced an overall spatial distribution of crossing locations and mean transit times closest to those observed.

Whilst the PT3 simulations, imposing a negative rheotaxis on the particles, reduced the duration of travel time between curtain C and D compared to PT1 (passive particles), they did not reduce this time as much as PT2 simulations (swimming on a constant bearing). This indicates that whilst the natural flow fields contribute to the modelled position of the particles and their curtain D crossing times/locations, it is active swimming at a constant bearing, which best predicts actual smolt migration pathway. Somewhat counter-intuitively, simulations PT3.2 (negative rheotaxis with a swimming speed of 0.168 m.s^{-1} when easterly velocity $>$0 m.s^{-1}.) and PT3.3 (negative rheotaxis with a swimming speed of 0.168 m s^{-1} only when easterly velocity $>$0 m.s^{-1} and northerly velocity $>$ 0 m.s^{-1}) lengthened the travel durations, relative to PT3.1. We hypothesized that by removing the behaviour during times of flood tide (dominantly south-west direction in the inner Moray Firth region) the degree of movement back into the inner Moray Firth would be reduced. This proved not to be the case; the tidal patterns in this region are likely to be more complex. This also shows how the natural flow fields do indeed have a role to play in the ultimate trajectory of the salmon smolts.

Discussion

Previous modelling of the migration of Atlantic salmon post-smolts in the first few weeks at sea indicated that migration was consistent with the fish following water currents and actively swimming in the direction of those currents (Mork *et al.*, 2012), which has also been supported by Atlantic salmon smolt tracking on the east coast of Canada (Ohashi and Sheng, 2018). Two realistic but alternative hypotheses might be that post-smolts disperse in random directions once they reach the open coast or, arguably more plausible is that they take the most direct marine route to their known feeding grounds in the Norwegian Sea. The study presented here did not support any of these three alternatives.

Post-smolts entering the Moray Firth made a clear and surprisingly consistent choice of migration direction. There was no evidence of random dispersal of post-smolts on reaching the coastal zone, with 70% of tagged post-smolts being detected in the 6 km at the south-east end of the 23 km curtain D. This pattern was consistent across individuals, over the period of the migration and across tidal cycles, indicating that these fish were making clear choices of their route of migration over the first few days following entry into the open coastal zone. The chosen migration direction is not the most direct route towards known feeding grounds in the Norwegian Sea, which would have taken them to the north-east on entering the coastal zone on a bearing of around 44°. In fact, no fish were detected crossing the outermost detection curtain within the most north-easterly 6 km section of curtain D. Rather, post-smolts migrating from the River Conon consistently used a migration route taking them almost directly east (ca 80°), and relatively close to the coast.

Unlike the directional current cues that smolts appear to use in riverine migration (Thorstad *et al.*, 2012), the present study indicates that migration direction is not simply the result of orientation downstream in a directional current for this population in the Moray Firth. However, it is clear that post-smolts are actively swimming. The passive particle tracking simulations clearly show that post-smolts are not swimming with the prevailing current but are, at least at times, swimming against the prevailing current. This current flows predominantly westwards (ca 220° from N) along the southern coast of the Moray Firth area of the inner firth to the west of Cullen (Adams and Martin, 1986; Hansom and

Black, 1996). Modelling of actively "swimming" particles shows that the best alignment of modelling and the empirical tracking occurs with smolts swimming at a speed of around 0.168 ms^{-1} (1.2 body lengths.s^{-1} for a 140 mm L_{F} fish) and on a course towards 70° from N.

Some partial support for the findings presented here is provided in two other studies. Moriarty *et al.* (2016) simulated Atlantic salmon post-smolt movements in the Gulf of Maine and similarly concluded that smolts were not passive drifting on marine currents. Thorstad *et al.* (2007) found that Atlantic salmon and anadromous brown trout (*Salmo trutta*) post-smolt movements in a Norwegian fjord also did not coincide with the water currents. Although we show that the migration of smolts in the present study is consistent with them swimming directionally on a fixed vector at a relatively fast swimming speed, it is not possible to determine if fish are migrating on a fixed bearing or if the determined bearing is a consequence of fish responding to other navigational cues.

The route taken by post-smolts in this study has the potential for some advantage. Further to the east (beyond the outermost curtain in this study), the predominant currents flow eastwards (Adams and Martin, 1986; Hansom and Black, 1996), which may be energetically favourable on later stages of the migration towards the known feeding grounds in the Norwegian Sea. The finding that post-smolt migration swimming is strongly directional is consistent with a recent modelling study by Ounsley *et al.* (2019), which showed that current-following behaviours did not facilitate outward migration from any of the modelled particle release locations on the Scottish coast. These authors showed that directed swimming behaviours (swimming speeds of 1–3 body lengths s^{-1} were tested) were needed during early migration for simulated post-smolts to successfully reach their marine feeding grounds. Although a recent study from Ireland has showed that smolts progressed through the Irish sea in a northerly trajectory at speeds of 0.5 body lengths s^{-1} over a maximum distance of 250 km ($n = 3$) and detections suggested the use of favourable ocean currents (Barry *et al.*, 2020).

Knowledge of post-smolt marine migration routes is essential to enable coastal zone management of activities, which have the potential to impact upon salmon post-smolts. Of particular importance is the rapid growth of offshore renewables in the British Isles (Esteban and Leary, 2012). Further insights into migratory behaviour in coastal waters could be gained through particle tracking experiments, which introduce additional but realistic variation in swimming speeds and behaviour and known coastal current patterns. For example, models could include vertical migration of the tracked particles. Although fish in this study remained within the top 5 m of water, Atlantic salmon are known to exhibit deeper diving behaviour.

Depending upon at what point in the marine migration this behaviour is initiated, it could result in potential interactions with any sea bed activities such as demersal fishing or sea bed development and construction. Tracking fish further out to sea than was achieved in this study may enable the identification of such behaviour in the marine environment. However, passive acoustic telemetry may not provide the most robust method for studying such behaviour.

Prediction of the migration patterns of Atlantic salmon smolts in the open sea distant from the coast presents further difficulties. An understanding of the details of the cues used by smolts and post-smolts to determine swimming direction, and thus

migration routes, are needed to populate the models. However, the approach adopted in the current study presented here provides one route through which this process might begin. The combination of smolt trawling surveys (Mork *et al.*, 2012), active tracking and particle tracking simulation are required to facilitate more informed model outputs. It is likely a better understanding of the fine scale drivers of navigation (e.g. currents, geomagnetism, salinity, resource availability) and where, when and how they are used, is required to refine our understanding of migration routes in the open ocean.

In common with other studies, the study presented here also showed that the loss rate during smolt migration was variable across habitat types. This effect may in part be the result of differential migration speeds as there was a non-significant ($p < 0.09$) trend for migration speed to predict loss rate. Generally, overall loss rates in this study were relatively low when compared with other studies (Table 1). Thorstad *et al.* (2012) in a review of studies up to that date, found Atlantic salmon smolt mortality ranging between 0.3–5% km^{-1} in freshwater, 0.6–36% km^{-1} in estuaries, and 0.8–3.4% km^{-1} in the marine environment. We found an average loss of 2.35% km^{-1} in freshwater, 0.32% km^{-1} in the estuary and 1.18% km^{-1} in the coastal marine environment (Moray Firth). The loss rate in the Moray Firth was slightly higher than the 0.8% km^{-1} found by Lacroix *et al.* (2005) for Atlantic salmon post-smolts in the Gulf of Maine. The mortality rate in the estuarine Cromarty Firth was low compared to that for freshwater-marine transitional zones reported in other studies (see Thorstad *et al.*, 2012), and lower than that in freshwater in the River Conon. Although observed detections of fish were slightly lower than the predicted detections, the general trend of high confirmed survival rates supports the conclusions. Localized reductions and the temporal reduction in efficiency (e.g. boat passing overhead) may coincide with smolt passage to reduce detection efficiency at that time, hence the slight reduction in observed detection compared to predicted detections at curtain C. The variation in loss rate estimates across different migration habitats is likely due to site-specific geographical features and predator assemblages. There may be multiple reasons for losses during smolt migration but those most commonly cited are a lack of physiological preparedness for transition between the fresh and saltwater environments and predation (Jarvi, 1989; Jepsen *et al.*, 2006; Thorstad *et al.*, 2012). If poor physiological preparedness for entry to sea water were the main influence mortality patterns then we might expect survival to be positively correlated with day of year (with later migrating smolts more likely to be physiologically prepared for sea entry) (Stich *et al.*, 2015) and a peak in losses soon after the entry to the marine environment. There was no evidence of either pattern in the current data strongly suggesting that this source of mortality was not a principal factor in this population. Although we have little direct evidence of this predation by birds, larger fish, and marine mammals could be an important factor in losses and such predators have been shown to have significant effects in other studies (Dieperink *et al.*, 2005; Svenning *et al.*, 2005; Blackwell and Juanes, 2011). This requires further investigation. Migration success was, however, predicted by the size of the group that was migrating on any day and by the migration time; with large groups and migration earlier in the migration period resulting in higher migration success.

Movement through the study system was fast and the smolts spent little time in the coastal zone, taking on average 8.1 ± 3.5 *SD* days to travel the ca. 62 km from the most upstream ALS to the most outer curtain D (a minimum speed of 7.7 $km.day^{-1}$). A pattern of fast movement through estuary and coastal areas towards the outer sea is frequently reported for Atlantic salmon smolts (e.g. Lefèvre *et al.*, 2012), however, there are also examples of smolts spending much longer time periods in coastal areas (e.g. >70 days in an inland sea).

What has not been reported previously is the tidal oscillation in migration direction seen in this study, 22% of fish made at least one detected movement in the direction opposite to seaward in the tidal estuary. These events were detected during flooding tides in the relatively constrained estuarine areas of the Cromarty Firth. Rapid migration into the coastal areas is often linked with higher survival (e.g. Renkawitz *et al.*, 2012).

The speed of migration differed between habitat types. Rate of movement was lowest in the lower freshwater reaches of the river where the current velocity is low, and highest within the inner Cromarty firth (A to B) where tides are likely constrained, with increased local water velocities, which may increase smolt movement speed. It is likely water velocities in this area are greater than smolt swimming ability since movement in both the upstream and downstream direction was faster than elsewhere in the study. The duration of residency events in the Cromarty Firth was significantly longer under a flooding tide than an ebb tide, possibly indicating fish persistently actively swimming in a seaward direction, i.e. swimming with the ebb tide but against the flood tide. The mean ROM in the Cromarty Firth ($0.32\,ms^{-1}$) was similar to other estimates of Atlantic salmon post-smolt movement in coastal areas (Kocik *et al.*, 2009: $0.28\,ms^{-1}$). The ROM has previously been correlated with tidal cycle (and currents), wind-induced currents (Fried *et al.*, 1978; Lacroix *et al.*, 2004; Stich *et al.*, 2015), barometric pressure, lunar illumination, cloud cover, and wave height (Fried *et al.*, 1978), and such relationships vary across studies. Given that tagged smolts are only detectable for a relatively short period of time when close to a receiver, combined with the heterogeneity of the environmental variables and small-scale, localized changes in conditions, it is difficult to identify common patterns of migration behaviour across study systems (Hedger *et al.*, 2008). This also highlights that the localized dynamics of the marine environment need to be considered as this may dictate the progression rate of smolts.

Changes in swimming depth of salmonids have been strongly related to temperature and salinity (Plantalech Manel-La *et al.*, 2009), and light conditions (Davidsen *et al.*, 2008). In this study, smolts were predominantly detected within the top 1 m of the water column and were detected higher in the water column at night than during the day. Smolt migration close to the water surface was also reported by Davidsen *et al.* (2008) who recorded individual mean depths of tagged smolts of <2.3 m and Renkawitz *et al.* (2012) who found 95% of daytime detections to be in <5 m depth. Similar preference for the near-surface habitat (<5 m depth) in coastal areas has also been found for adult Atlantic salmon (Godfrey *et al.*, 2015). Few studies have explored diurnal effects during coastal migration but those that have, report results similar to this study (Reddin and Short, 1991; Davidsen *et al.*, 2008; Hedger *et al.*, 2008). The greater variability in depth during daylight may be due to fish actively foraging since they rely on visual cues to identify prey (Davidsen *et al.*, 2008; Hedger *et al.*, 2008; Renkawitz *et al.*, 2012), or avoiding predators (Reddin and Short, 1991).

The results from the study presented here indicate that salmon post-smolts in the nearshore coastal zone actively swim along preferred migration routes that these routes are not directly predicted by simple current direction and speed and, at least at times, do not align with the most logical direct route to know feeding grounds.

Supplementary data

Supplementary material is available at the *ICESJMS* online version of the manuscript.

Data availability

The data underlying this article will be shared on reasonable request to the corresponding author.

References

Adams, J. A., and Martin, J. H. A. 1986. The hydrography and plankton of the Moray Firth. Proceedings of the Royal Society of Edinburgh, 91B: 37–56.

Alerstam, T., Hedenström, A., and Åkesson, S. 2003. Long-distance migration: evolution and determinants. Oikos, 103: 247–260.

Barry, J., Kennedy, R. J., Rosell, R., and Roche, W. K. 2020. Atlantic salmon smolts in the Irish Sea: first evidence of a northerly migration trajectory. Fisheries Management and Ecology, 27: 517–522.

Bartoń, K. 2016. MuMIn: Multi model inference. Package for R. Current version at https://cran.r-project.org/web/packages/MuMIn/MuMIn.pdf (last accessed 11 February 2021).

Bivand, R., and Lewin-Koh, N. 2016. Maptools: tools for reading and handling spatial objects. https://CRAN.R-project.org/package=maptools (last accessed 11 February 2021).

Blackwell, B. F., and Juanes, F. 2011. Predation on Atlantic Salmon smolts by striped bass after dam passage. North American Journal of Fisheries Management, 14: 4.

Breece, M. W., Fox, D. A., and Oliver, M. J. 2018. Environmental drivers of adult Atlantic sturgeon movement and residency in Delaware Bay. Marine and Coastal Fisheries: dynamics. Management and Ecosystem Science, 10: 269–280.

Campbell, H. A., Watts, W. E., Dwyer, R. G., and Franklin, C. E. 2012. V-Track: software for analysing and visualising animal movement from acoustic telemetry detections. Marine and Freshwater Research, 63: 815–820.

Campbell, L. 2018. Hydrodynamic Modelling of the Moray Firth, Marine Alliance for Science and Technology for Scotland Numerical & Experimental Hydrodynamic Modelling Forum Workshop, 19 April 2018, Grassmarket Centre Edinburgh, 86 Candlemaker Row, EH1 2QA. https://www.masts.ac.uk/research/research-forums/numerical-experimental-hydrodynamic-modelling-forum/nehm-2018-workshop-presentations/ (last accessed 11 February 2021).

Chaput, G., Carr, J., Daniels, J., Tinker, S., Jonsen, I., and Whoriskey, F. 2019. Atlantic salmon (*Salmo salar*) smolt and early post-smolt migration and survival inferred from multi-year and multi-stock

acoustic telemetry studies in the Gulf of St. Lawrence, northwest Atlantic. ICES Journal of Marine Science, 76: 1107–1121.

Chen, C., Beardsley, R., Cowles, G., Qi, J., Lai, Z., Gao, G., Stuebe, D. et al. 2011 An unstructured grid, Finite-volume coastal ocean model, FVCOM User Manual. https://wiki.fvcom.pml.ac.uk/lib/exe/fetch.php?media=source:fvcom_small.pdf (last accessed 11 February 2021).

Chen, C., Liu, H., and Beardsley, R. C. 2003. An unstructured grid, finite-volume, three-dimensional, primitive equations ocean model: application to coastal ocean and estuaries. Journal of Atmospheric and Oceanic Technology, 20: 159–186.

Cresswell, K. A., Satterthwaite, W. H., and Sword, G. A. 2011. Understanding the evolution of migration through empirical examples. Animal Migration: A Synthesis, pp. 7–16. Ed. by E.J. Milner-Gulland, J.M. Fryxell and A.R.E. Sinclair. Oxford University Press, Oxford. 280 pp.

Cooke, S. J., Hinch, S. G., Wikelski, M., Andrews, R. D., Kuchel, L. J., Wolcott, T. G., and Butler, P. J. 2004. Biotelemetry: a mechanistic approach to ecology. Trends in Ecology and Evolution, 19: 334–343.

Cooke, S. J., Midwood, J. D., Thiem, J. D., Klimley, P., Lucas, M. C., Thorstad, E. B., Eiler, J. et al. 2013. Tracking animals in freshwater with electronic tags: past, present and future. Animal Biotelemetry, 1: 5.

Cooke, S. J., and Thorstad, E. B. 2011. Is Radio Telemetry Getting Washed Downstream? The Changing Role of Radio Telemetry in Studies of Freshwater Fish Relative to other Tagging and Telemetry Technology, American Fisheries Society Symposium. 76: 349–369.

Davidsen, J. G., Plantalech Manel-La, N., Økland, F., Diserud, O. H., Thorstad, E. B., Finstad, B., Sivertsgård, R. et al. 2008. Changes in swimming depths of Atlantic salmon *Salmo salar* post-smolts relative to light intensity. Journal of Fish Biology, 73: 1065–1074.

De Dominicis, M., O'Hara Murray, R., Wolf, J., and Gallego, A. 2018. The Scottish Shelf Model 1990 – 2014 climatology version 2.01. https://data.marine.gov.scot/dataset/scottish-shelf-model-1990-%E2%80%93-2014-climatology-%E2%80%93-reduced-precision-output-version-201/resource (last accessed 11 February 2021).

Dee, D. P., Uppala, S. M., Simmons, A. J., Berrisford, P., Poli, P., Kobayashi, S., Andrae, U. et al. 2011. The ERA-Interim reanalysis: configuration and performance of the data assimilation system. Quarterly Journal of the Royal Meteorological Society, 137: 553–597.

Dieperink, C., Bak, B. D., Pedersen, L.-F., Pedersen, M. I., and Pedersen, S. 2005. Predation on Atlantic salmon and sea trout during their first days as postsmolts. Journal of Fish Biology, 61: 848–852.

Dingle, H. 2014. Migration: The Biology of Life on the Move. Oxford University Press, New York.478 pp.

Eek, D., and Bohlin, T. 1997. Strontium in scales verifies that sympatric sea-run and stream-resident brown trout can be distinguished by coloration. Journal of Fish Biology, 51: 659–661.

Edwards, K. P., Barciela, R., and Butenschön, M. 2012. Validation of the NEMO-ERSEM operational ecosystem model for the North West European continental shelf. Ocean Science, 8: 983–1000.

Esteban, M., and Leary, D. 2012. Current developments and future prospects of offshore wind and ocean energy. Applied Energy, 90: 128–136.

Fried, S. M., McCleave, J. D., and LaBar, G. W. 1978. Seaward migration of hatchery-reared Atlantic Salmon, *Salmo salar*, smolts in the Penobscot river estuary, Maine: riverine movements. Journal of the Fisheries Research Board of Canada, 35: 76–87.

Gauld, N. R., Campbell, R. N. B., and Lucas, M. C. 2013. Reduced flow impacts salmonid smolt emigration in a river with low-head weirs. Science of the Total Environment, 458: 435–443.

Godfrey, J. D., Stewart, D. C., Middlemas, S. J., and Armstrong, J. D. 2015. Depth use and migratory behaviour of homing Atlantic salmon (*Salmo salar*) in Scottish coastal waters. ICES Journal of Marine Science, 72: 568–575.

Halttunen, E., Rikardsen, A. H., Davidsen, J. G., Thorstad, E. B., and Dempson, J. B. 2009. Survival, migration speed and swimming depth of Atlantic salmon kelts during sea entry and fjord migration. Tagging and tracking of marine animals with electronic devices, pp. 35–49. *In* Tagging and Tracking of Marine Animals with Electronic Devices. Ed. by J. L. Nielsen, H. Arrizabalaga, N. Fragoso, A. Hobday, M. Lutcavage, and J. S. Dordrecht. Springer, Dordrecht.

Hansom, H.D. and Black, D.LK. 1996. Coastal processes and management of Scottish estuaries. 2: Estuaries of the Outer Moray Firth. Scottish Natural Heritage, Edinburgh. 92 pp.

Hasler, A. D. 1966. Underwater Guideposts. The University of Wisconsin Press, Madison, WI.

Hayden, T. A., Holbrook, C. M., Binder, T. R., Dettmers, J. M., Cooke, S. J., Vandergoot, C. S., and Kruegar, C. C. 2016. Probability of acoustic transmitter detections by receiver lines in Lake Huron: results of multi-year field tests and simulations. Animal Biotelemtry, 4: 19.

Hedger, R. D., Martin, F., Hatin, D., Caron, F., Whoriskey, F. G., and Dodson, J. J. 2008. Active migration of wild Atlantic salmon *Salmo salar* smolt through a coastal embayment. Marine Ecology Progress Series, 355: 235–246.

Heupel, M. R., Semmens, J. M., and Hobday, A. J. 2006. Automated acoustic tracking of aquatic animals: scales, design and deployment of listening station arrays. Marine and Freshwater Research, 57: 1–13.

Hoar, W. S. 1988. The physiology of smolting Salmonids. Fish Physiology, 11(B): 275–343.

Hodder, K. H., Masters, J. E. G., Beaumont, W. R. C., Gozlan, R. E., Pinder, A. C., Knight, C. M., and Kenward, R. E. 2007. Techniques for evaluating the spatial behaviour of river fish. Hydrobiologia, 582: 257–269.

Honkanen, H. M., Rodger, J. R., Stephen, A., Adams, K., Freeman, J., and Adams, C. E. 2018. Counterintuitive migration patterns by Atlantic salmon Salmo salar smolts in a large lake. Journal of Fish Biology, 93: 159–162.

Hussey, N. E., Kessel, S. T., Aarestrup, K., Cooke, S. J., Cowley, P. D., Fisk, A. T., Harcourt, R. G. *et al.* 2015. Aquatic animal telemetry: a panoramic window into the underwater world. Science, 348: 1255642.

ICES. 2019. North Atlantic Salmon Stocks. In Report of the ICES Advisory Committee, 2019. ICES Advice 2019. http://ices.dk/sites/pub/Publication%20Reports/Advice/2019/2019/sal.oth.nasco.pdf (last accessed 11 February 2021).

Jarvi, T. 1989. Synergistic effect on mortality in Atlantic salmon, *Salmo salar*, smolt caused by osmotic stress and presence of predators. Environmental Biology of Fishes, 26: 149–152.

Jepsen, N., Holthe, E., and Økland, F. 2006. Observations of predation on salmon and trout smolts in a river mouth. Fisheries Management and Ecology, 13: 341–343.

Lacroix, G. L., Knox, D., and Stokesbury, M. J. W. 2005. Survival and behaviour of post-smolt Atlantic salmon in coastal habitat with extreme tides. Journal of Fish Biology, 66: 485–498.

Lacroix, G. L., McCurdy, P., and Knox, D. 2004. Migration of Atlantic Salmon postsmolts in relation to habitat use in a coastal system. Transactions of the American Fisheries Society, 133: 1455–1471.

Kocik, J. F., Hawkes, J. P., Sheehan, T. F., Music, P. A., and Beland, K. F. 2009. Assessing estuarine and coastal migration and survival of wild Atlantic salmon smolts from the Narraguagus River, Maine using ultrasonic telemetry. In American Fisheries Society Symposium. 69: 293–310.

Lefèvre, M. A., Stokesbury, M. J. W., Whoriskey, F. G., and Dadswell, M. J. 2012. Migration of Atlantic salmon smolts and post-smolts in the Riviere Saint-Jean, QC north shore from riverine to marine ecosystems. Environmental Biology of Fishes, 96: 1017–1028.

Liu, C., Cowles, G. W., Churchill, J. H., and Stokesbury, K. D. E. 2015. Connectivity of the bay scallop (*Argopecten irradians*) in Buzzards Bay, Massachusetts, U.S.A. Fisheries Oceanography, 24: 364–382.

Lucas, M. C., and Baras, E. 2000. Methods for studying spatial behaviour of freshwater fishes in the natural environment. Fish and Fisheries, 1: 283–316.

Minkoff, D., Putman, N. F., Atema, J., and Ardren, W. R. 2020. Nonanadromous and anadromous Atlantic salmon differ in orientation responses to magnetic displacements. Canadian Journal of Fisheries and Aquatic Sciences, 77: 1846–1852.

Moriarty, P. E., Byron, C. J., Pershing, A. J., Stockwell, J. D., and Xue, H. 2016. Predicting migratory paths of post-smolt Atlantic salmon (*Salmo salar*). Marine Biology, 163: Article 74.

Mork, K. A., Gilbey, J., Hansen, L. P., Jensen, A. J., Jacobsen, J. A., Holm, M., Holst, J. C. *et al.* 2012. Modelling the migration of post-smolt Atlantic salmon (*Salmo salar*) in the Northeast Atlantic. ICES Journal of Marine Science, 69: 1616–1624.

NASCO 2011 Advancing understanding of Atlantic salmon at sea: Merging genetics and ecology to resolve Stock-specific migration and distribution patterns, SALSEA-Merge. http://www.nasco.int/sas/pdf/salsea_documents/salsea_merge_finalreports/Completed Final Report SALSEA-Merge.pdf (last accessed 31 January 2017).

O'Dea, E. J., Arnold, A. K., Edwards, K. P., Furner, R., Hyder, P., Martin, M. J., Siddorn, J. R. *et al.* 2012. An operational ocean forecast system incorporating NEMO and SST data assimilation for the tidally driven European North-West shelf. Journal of Operational Oceanography, 5: 3–17.

Ohashi, K., and Sheng, J. 2018. Study of Atlantic salmon post-smolt movement in the Gulf od St. Lawrence using an individual-based model. Regional Studies in Marine Science, 24: 113–132.

Okubo, A. 1971. Oceanic diffusion diagrams. Deep-Sea Research, 18: 789–802.

Ounsley, J., Gallego, A., Morris, D., and Armstrong, J. 2019. Regional variation in directed swimming by Atlantic salmon smolts leaving Scottish waters for their oceanic feeding grounds—a modelling study. ICES Journal of Marine Science, 77: 315–325.

Plantalech Manel-La, N., Thorstad, E. B., Davidsen, J. G., Økland, F., Sivertsgård, R., Mckinley, R. S., and Finstad, B. 2009. Vertical movements of Atlantic salmon post-smolts relative to measures of salinity and water temperature during the first phase of the marine migration. Fisheries Management and Ecology, 16: 147–154.

Putman, N. F., Jenkins, E. S., Michielsens, C. G. J., and Noakes, D. L. G. 2014. Geomagnetic imprinting predicts spatio-temporal variation in homing migration of pink and sockeye salmon. Journal of the Royal Society Interface, 11: 20140542.

Quinn, T. P., Terhart, B. A., and Groot, C. 1989. Migratory orientation and vertical movements of homing adult sockeye salmon, *Oncorhynchus nerka*, in coastal waters. Animal Behaviour, 37: 587–599.

R Core Team. 2016. R: A Language and Environment for Statistical Computing. R Foundation for Statistical Computing, Vienna, Austria.

Rankin, M. A., and Burchsted, J. C. A. 1992. The cost of migration in insects. Annual Review of Entomology, 37: 533–559.

Reddin, B. G., and Short, P. B. 1991. Postmolt Atlantic salmon (*Salmo salar*) in the Labrador Sea. Canadian Journal of Fisheries and Aquatic Sciences, 48: 2–6.

Renkawitz, M. D., Sheehan, T. F., and Goulette, G. S. 2012. Swimming depth, behavior, and survival of Atlantic salmon post-smolts in Penobscot Bay, Maine. Transactions of the American Fisheries Society, 141: 1219–1229.

Rikardsen, A. H., and Dempson, J. B. 2011. Dietary life-support: the food and feeding of Atlantic salmon at sea. *In* Atlantic Salmon Ecology, pp. 115–143. Ed. by A. Oystein, S. Einum, A. Klemetsen, and S. Skurdal. Blackwell, Oxford.

Sloat, M. R., and Reeves, G. H. 2014. Individual condition, standard metabolic rate, and rearing temperature influence steelhead and rainbow trout(*Oncorhynchus mykiss*) life histories. Canadian Journal of Fisheries and Aquatic Sciences, 71: 491–501.

. Coastal processes and management of Scottish estuaries. 1: The Dornoch, Cromarty and Beauly/Inverness Firths. Scottish Natural Heritage, Edinburgh. 99 pp.

Stich, D. S., Zydlewski, G. B., Kocik, J. F., and Zydlewski, J. D. 2015. Linking behavior, physiology, and survival of atlantic salmon smolts during estuary migration. Marine and Coastal Fisheries, 7: 68–86.

Svenning, M.-A., Borgstrøm, R., Dehli, T. O., Moen, G., Barrett, R. T., Pedersen, T., and Vader, W. 2005. The impact of marine fish predation on Atlantic salmon smolts (*Salmo salar*) in the Tana estuary, north Norway, in the presence of an alternative prey, lesser sandeel (*Ammodytes marinus*). Fisheries Research, 76: 466–474.

Thorstad, E., Kland, F., Finstad, B., Sivertsgrd, R., Bjorn, P., and McKinleyd, R. 2004. Migration speeds and orientation of Atlantic salmon and sea trout post-smolts in a Norwegian fjord system. Environmental Biology of Fishes, 71: 305–311.

Thorstad, E. B., Økland, F., Finstad, B., Sivertsga, R., Plantalech, N., Bjørn, P. A., and Mckinley, R. S. 2007. Fjord migration and survival of wild and hatchery-reared Atlantic salmon and wild brown trout post-smolts. Hydrobiologia, 582: 99–107.

Thorstad, E. B., Rikardsen, A. H., Alp, A., and Økland, F. 2013. The use of electronic tags in fish research—an overview of fish telemetry methods. Turkish Journal of Fisheries and Aquatic Sciences, 13: 881–896.

Thorstad, E. B., Whoriskey, F., Uglem, I., Moore, A., Rikardsen, A. H., and Finstad, B. 2012. A critical life stage of the Atlantic salmon *Salmo salar*: behaviour and survival during the smolt and initial post-smolt migration. Journal of Fish Biology, 81: 500–542.

Wolf, J., Yates, N., Brereton, A., Buckland, H., De Dominicis, M., Gallego, A., and O'Hara Murray, R. 2016. The Scottish shelf model. Part 1: shelf-wide domain. Scottish Marine and Freshwater Science Vol 7 No 3. Marine Scotland Science, Edinburgh. 155 pp.

Zuur, A. F., Ieno, E. N., Walker, N., Saveliev, A. A., and Smith, G. M. 2009. Mixed Effects Models and Extensions in Ecology with R. Springer New York (Statistics for Biology and Health), New York, NY.

Handling editor: Jonathan Grabowski